MODELING BREAKDOWN IN RF CAVITIES USING PARTICLE-IN-CELL (PIC) CODES*

S. Mahalingam†, J.R. Cary, P.H. Stoltz, S.A. Veitzer, Tech-X Corporation, Boulder, CO 80303, USA

Abstract

A main limitation on the design of future accelerators is breakdown of metallic structures. We have developed computer models of the process of breakdown using Particle-In-Cell (PIC) codes. We use the plasma simulation package OOPIC Pro, a two dimensional electromagnetic code, to self-consistently model the breakdown. We describe here the results of our numerical experiments, including sensitivity of breakdown triggers on field emission parameters, and the potential to measure the onset of breakdown by examining impurity radiation. We also report our work on enhancing the parallel capabilities available in the OOPIC Pro code which allows plasma simulations to run on multiple processors with distributed memory.

INTRODUCTION

Future accelerator projects [1] desire to use large electric fields ($>$ 50 MV/m) coupled with high magnetic fields ($>$ 2.5 T) for generating high intensity muon beams required for the production of high-energy neutrinos. These large fields will reduce the number of costly focusing elements needed for limiting the muon beam emittance. However, metallic structures often break down when operating with such large field gradients. Breakdown processes in RF cavities have been experimentally studied by many researchers, for instance, [2]-[4] have recently studied breakdown in 805 MHz and 200 MHz copper cavities. Breakdown limits in acclerating structures [4] are presently the main constraint on the electric field strength in muon cooling designs. We have developed computer models to study breakdown using OOPIC Pro [5]. OOPIC Pro is a 2-Dimensional Particle-in-Cell (PIC) code that is being used by plasma physicists and engineers for modeling various plasma problems. OOPIC Pro self-consistently solves the interactions of fields and particles and adopts a kinetic particles to model the plasma.

BREAKDOWN MODEL

A series of recent experiments [2]- [4] have resulted in a theory of breakdown processes involved in metallic structures like those used for muon cooling. The theory postulates that stresses induced by electric fields exceed the tensile strength of surface materials and this results in fragments of surface material being pried loose. These metal fragments are then broken apart, excited and ionized by field emitted electrons resulting in a high density plasma of impurities. This plasma radiates away energy as photons, resulting in adsorption of RF power. Also the impurity copper ions that impact cavity surfaces can cause secondary emission of electrons and physical sputtering of wall material. These processes lead to an avalanche of plasma impurity production inside the cavity. Eventually with RF power being taken away by radiation and coupled with the erosion processes of cavity surfaces, an arc may form, causing physical damage to the cavity structures.

The main features in our computational model are field-emission of electrons, electron-impact ionization of neutrals, ion-induced secondary emission of electrons, ion-induced sputtering of neutral atoms, plasma radiation effects, and surface heating due to bombardment of charged particles. Details of these features are presented in Reference [6]. Prior computational breakdown models [7] using OOPIC Pro, did not consider the following physical processes: ion-induced sputtering, ion-induced secondary emission and plasma radiation. We have enabled these features into the OOPIC Pro package by interfacing it with TxPhysics [8]. TxPhysics is a cross-platform numerical library composed of various physical process modules.

Breakdown is modeled by considering a conical asperity in the cavity surface with a surrounding background copper gas of near solid density. This is similar to the situation imagined by Norem et. al. [2]. Figure 1 shows the 2-D breakdown simulation geometry and physical dimensions considered in OOPIC Pro. We used 0.2 μm square computational cells with a 0.01 ps time step. The time step is chosen to keep particles from crossing more than one computational cell per step. We use macro particles in our simulations, so each simulated particle represents 50 physical particles.

Numerically, the conical defect itself is stair-stepped into 5 segments to align the emitting surface with the computational grid. An electric field is applied through an external RF source with a frequency of 805 MHz. The magnitude of the electric fields are in the range 20 to 60 MV/m. We consider a field enhancement factor, $\beta_{FN} = 184$, as estimated by Norem et. al [2], in our Fowler-Nordheim field emission model. The Fowler-Nordheim emission depends on the net surface field, including contributions from both the applied RF signal and the space-charge fields of the plasma particles.

RESULTS

Simulation results for a background gas pressure of 35 torr and the effects of applied external magnetic fields can be found in [6]. We present here numerical results for a

* Work supported by US Department of Energy under Small Business Innovation Research Contract DE-FG02-07ER84833

† sudhakar@txcorp.com

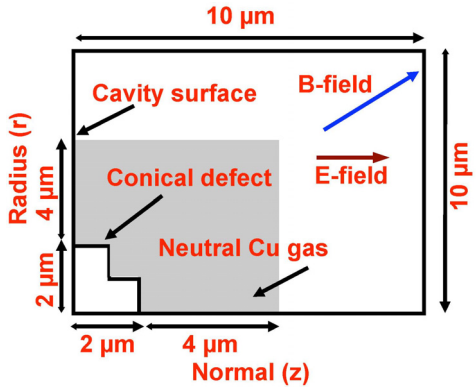

Figure 1: Two dimensional breakdown simulation geometry.

critical background gas pressure study.

In our simulations, a breakdown event is believed to occur when there is a large build up of plasma particles. One of the main factors that triggers such a large build up of plasma particles in the simulation is the background copper gas density. When the rate of impact ionization by field emitted electrons increases, there is a build up of plasma in the cavity. However, there is a critical background gas density below which the rate of ion production via impact ionization is too low to sustain a buildup of plasma and to trap field-emitted electrons. Numerically we determine this critical pressure by observing the time evolution of different particle species' for various pressure cases. If a breakdown event does not occur after 1 μs of simulation time, corresponding to approximately 100 million steps, we believe that we are below this critical level. For this study we ignore the applied external magnetic fields. We have found that the critical background gas pressure is somewhere between 25 torr and 35 torr, corresponding to a density range of 8.6×10^{23} to 12×10^{23} particles/m^3.

Figure 2 shows the total number of physical particles in a typical breakdown simulation with a background gas pressure of 25 torr. There are more than 250 RF cycles in this simulation. None of the particle species' builds up over time. Initially for a few RF cycles (6 ns), the number of ions increases rapidly. After 6 ns, the number of ions in the simulation oscillates over consistent upper and lower limits, depending on the increase or decrease in the number of field-emitted electrons. The current density from field-emitted electrons is a strong function of the electric field normal at the emitting surface. At the defect, electric fields due to space charge are smaller when there is no build up of plasma. Thus the number of field emitted electrons in the simulation is not increasing over time. These field-emitted electrons are not sufficient to increase the rate of impact ionization of the background gas. For the same reason, the number of ionization electrons is smaller. The number of secondary emission electrons from the cavity surface is small because ions are moving away from the cavity surface due to insufficient build up of plasma near the defect region. No physical sputtering of wall material occurs for the same reason.

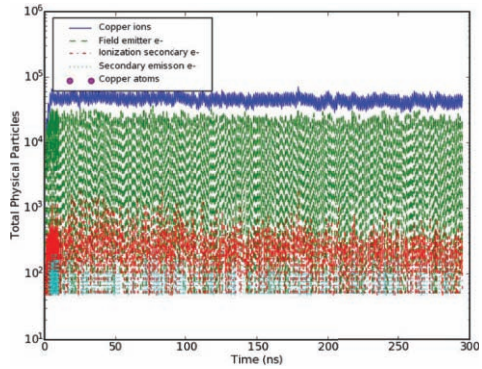

Figure 2: Total number of physical particles for a background gas pressure of 25 torr.

For comparison the the above case, figure 3 shows the total number of physical particles in a typical breakdown simulation with a background gas pressure of 35 torr. There are four RF cycles in this simulation before breakdown occurs. The total number of ions increases after each RF cycle, and the rate of ionization of the background copper gas also increases. After the third RF cycle period (3.6 ns), the number of field emitted electrons and the number of secondary electrons from ionization collisions does not completely drop to zero as in the previous two RF cycles, because these electrons are trapped by the electric potential of the copper ions in the plasma. The total number of secondary emission electrons from the cavity surface is small compared to the total number of other electron species because the number of ions striking the cavity walls is small at such short time scales. Physical sputtering of wall material occurs only after the third RF cycle for the same reason.

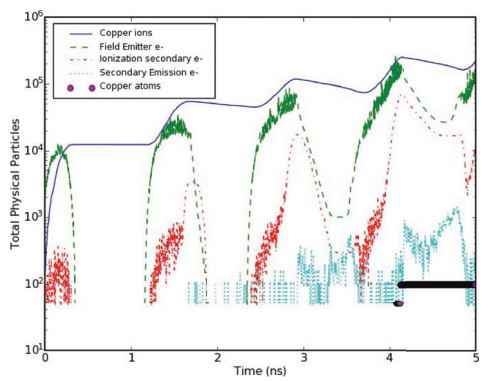

Figure 3: Total number of physical particles for a background gas pressure of 35 torr.

Figure 4 shows the continuum and line radiated power results for a background gas pressure of 25 torr. As is seen for physical particles in figure 2, both continuum and line radiated power does not build up over time. The oscillations of radiated power are due to the oscillations of total

density of both electron and ion particles in the simulation. The line radiated power is three orders of magnitude larger than the maximum continuum radiated power. This is because the temperature of the plasma in our simulations is low ($<$ 100 eV) and because the line radiated power is inversely proportional to the square root of the temperature.

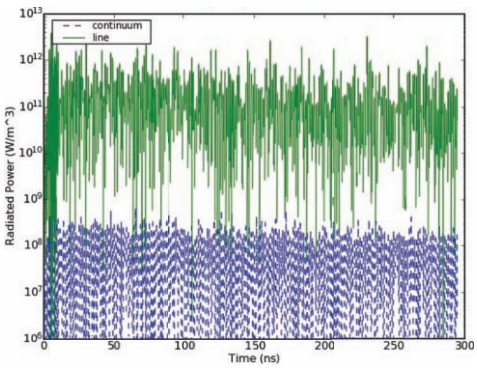

Figure 4: Continuum and line radiated power in W/m^3 with a background gas pressure of 25 torr

Similarly for comparison of above results, figure 5 shows the radiated power results for a background gas pressure of 35 torr. Both continuum and line radiated power continues to increase after 3.6 ns due to the increased density of both electron and ion particles in the simulation (see figure 3).

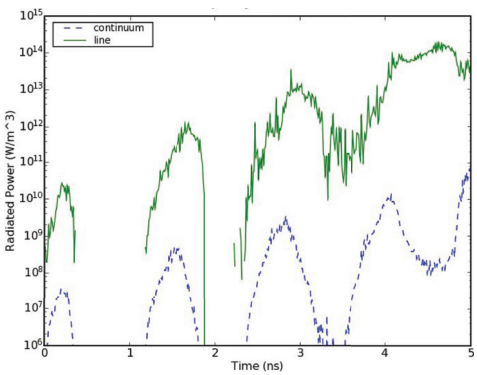

Figure 5: Continuum and line radiated power in W/m^3 with a background gas pressure of 35 torr.

PARALLEL OOPIC PRO

Previously, OOPIC Pro supported only parallel electromagnetic (EM) algorithms which allowed plasma simulations to run on multiple processors [9]. No parallel electrostatic (ES) solver had been implemented. Thus the parallel feature in OOPIC Pro did not allow one to take advantage of using electrostatic algorithms to solve electrostatic problems. In an ES problem, one can often select a time step that is an order of magnitude bigger than the corresponding EM time step, which is typically limited by the Courant condition. We have developed a parallel Poisson solver, and implemented into OOPIC Pro as part of this work. This new feature in OOPIC Pro allows researchers to obtain electrostatic simulation results quicker.

For the parallel ES simulation, the charge density and electric field information is exchanged along the partitioned boundary nodes. We also implemented interface calls to standard PETSc libraries to solve Poisson's equation in order to compute the electric potential in parallel ES simulations.

We simulated a conducting box 10 cm long and 2 cm heigh which is initially loaded with a uniform plasma of argon ions and electrons. A uniform computational mesh with 1024 grid points both in the x and y directions is used. The simulation time step is 0.5 ps and we performed 5000 time steps. Charged particles are loaded with a plasma density of $1 \times 10^{10} m^{-3}$ in the computational domain. More than one million grid points and approximately one million computer particles are considered in this problem.

Figure 6 shows the speed up results obtained from the parallel OOPIC Pro simulation (in solid lines) and the perfect speed up curve (in dashed lines). A speed up is observed with respect to the number of processors. However, it is slightly affected for number of processors $>$16. This happens because of the global nature of Poisson equation which require more inter processor communications for field solving when large number of processors used in the simulations.

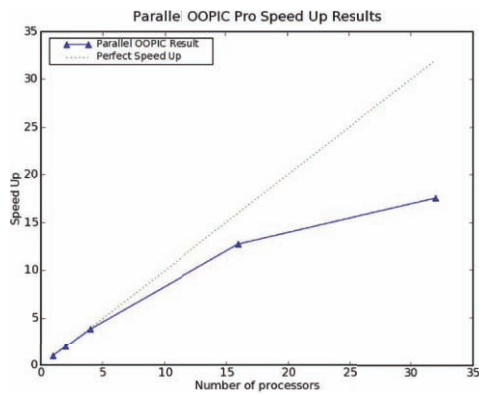

Figure 6: Parallel performance of OOPIC Pro for an electrostatic plasma problem.

REFERENCES

[1] M. Alsharo'a, *et al.*, Phys. Rev. ST-AB, **6**, 081001, 2003.

[2] J. Norem, *et al.*, Phys. Rev. ST-AB, **6**, 072001, 2003.

[3] A. Moretti *et al.*, Phys. Rev. ST-AB, **8**, 072001, 2005.

[4] A. Hassanein, *et al.*, Phys. Rev. ST-AB, **9**, 062001, 2006.

[5] D.L. Bruhwiler *et al.*, Phys. Rev. ST-AB, **4**, 101302, 2001.

[6] S. Mahalingam, S.A. Veitzer, P.H. Stoltz, Proceedings of IEEE IPMC and HV Workshop, Las Vegas, NV, May 2008.

[7] G. Werner, Ph.D. Dissertation, Cornell University, 2004.

[8] TxPhysics Users Manual, `http://txphysics.txcorp.com`.

[9] P.J. Mardahl, Ph. D. Dissertation, University of California, Berkeley, CA, 2001.